Environ. Sci. Technol. 2009 43, 9161–9166

Single-Walled Carbon Nanotubes Exhibit Limited Transport in Soil Columns

DEB P. JAISI[†,‡] AND MENACHEM ELIMELECH*[,†]

Department of Chemical Engineering, Environmental Engineering Program, Yale University, New Haven, Connecticut 06520-8286, and Department of Geology and Geophysics, Yale University, New Haven, Connecticut 06520-8109

Received June 30, 2009. Revised manuscript received October 3, 2009. Accepted October 27, 2009.

The increased production and commercial use of nanomaterials combined with a lack of regulation to govern their disposal may result in their introduction to soils and ultimately into groundwater systems. In this study, we investigated the transport behavior of carboxyl-functionalized single-walled carbon nanotubes (SWNTs) in columns packed with a natural soil. In general, SWNT deposition (filtration) rate increased with increasing solution ionic strength, with divalent cations (Ca^{2+}) being more effective in increasing SWNT retention than monovalent cations (K^+). However, SWNT deposition rate over a very wide range of monovalent and divalent cation concentrations (0.03 to 100 mM) was relatively high and changed only slightly above 0.3 mM KCl or 0.1 mM $CaCl_2$. In contrast, filtration of another type of engineered carbon-based nanomaterial, namely aqueous fullerene (C_{60}) nanoparticles (radius of 51 nm), was more sensitive to solution ionic strength, displaying lower deposition rate and more effective transport in soil than SWNTs. These observations indicate that physical straining governs SWNT filtration and transport under all the solution chemistries investigated in the present study. It is proposed that SWNT shape and structure, particularly the very large aspect ratio and its highly bundled (aggregated) state in aqueous solutions, as well as the heterogeneity in soil particle size, porosity, and permeability, collectively contribute to straining in flow through soil media. Our results suggest that SWNTs of comparable properties to those used in the present study will not exhibit substantial transport and infiltration in soils because of effective retention by the soil matrix.

Introduction

Carbon nanotubes (CNTs) are a class of nanomaterials that possess unique size- and structure-dependent optical, electronic, magnetic, thermal, chemical, and mechanical properties (*1*, *2*). These exceptional properties prompt the use of CNTs in numerous technological applications, such as fabrication of superconductors, optical and storage devices, fuel cells, sensors, and catalysts (*3*). The potential widespread use of CNTs along with a lack of regulation governing their disposal leave a gap for their possible release into the environment (*4*).

CNTs released into soils and sediments may eventually find their way into groundwater, reservoirs, and river systems and, thereby, may enter into the food chains of living organisms (*5*). Furthermore, CNTs are some of the least biodegradable synthetic materials (*6*), are insoluble in water in pristine form (*6*), and are reported to be toxic to bacteria (*7*) and human cells (*8*). Calls for more reliable data on the behavior of nanomaterials in the environment and possible health effects have come from government agencies and environmental advocacy groups (*9*). The emerging nanomaterial industry has also expressed the need for research on potential risks associated with nanomaterials as a mean of reducing barriers to market acceptance and to limit potential liabilities. These concerns demand a thorough understanding of the fate and mobility of CNTs, including the mechanisms of filtration (deposition) and remobilization in subsurface environments. This information, in turn, will be useful for developing regulatory guidelines for disposal facilities, such as repositories and landfills.

The mobility of colloidal particles in porous media and the factors that control their transport and filtration (deposition) have been studied extensively in model laboratory systems, particularly for cases involving silica, latex, bacteria, natural colloids, and iron oxide particles (e.g., refs *10*−*14*). However, despite a large number of publications that describe the synthesis of nanoparticles of a specific size, shape, and composition, only recently have there been a few studies that describe the transport and deposition of several types of carbon-based nanoparticles, including fullerenes, in packed columns (*15*−*19*). Moreover, studies involving fate and transport of CNTs in natural soil media are virtually nonexistent.

Soils are quite different than model porous media or aquifer materials commonly used in laboratory column experiments in terms of physical and chemical properties that may influence the filtration and transport of CNTs. Soil media also exhibit large variability in the shape, size, and roughness of mineral particles; composition and relative proportion of minerals; surface charge properties of minerals; and size distribution and interconnectivity of pores among minerals. Additionally, soil surface properties may change as a result of specific interactions with sorbed ions, organic coating, and mineral precipitates on grain surfaces. Because of the inherent physical and chemical heterogeneities in soils, results obtained from sorted aquifer materials, model porous media, or theoretical models cannot be used to extrapolate or predict transport of CNTs in natural soil media. To better understand the transport behavior of CNTs in subsurface environments, it is imperative to carry out experiments using columns packed with natural soils.

In this paper we investigate the transport behavior of single-walled carbon nanotubes (SWNTs) in soils under saturated flow conditions. A laboratory-scale column packed with natural soils was used to study the retention of SWNTs under a wide range of aqueous solution chemistries. Selected column experiments with monodisperse, spherical fullerene (C_{60}) nanoparticles were also carried out to explain and validate key SWNT deposition mechanisms. Our results suggest that SWNT mobility in soils is limited because of the irregular shape and large aspect ratio of SWNTs, as well as the large variability in particle size, porosity, permeability, and pore interconnectivity of natural soil media that promote SWNT retention by physical straining.

* Corresponding author phone: (203) 432-2789; e-mail: menachem.elimelech@yale.edu.
[†] Department of Chemical Engineering.
[‡] Department of Geology and Geophysics.

10.1021/es901927y CCC: $40.75
Published on Web 11/11/2009

Materials and Methods

Preparation of SWNTs and Fullerenes. Carboxyl (COOH)-functionalized SWNTs were purchased from Cheap Tubes Inc. (Brattleboro, VT). Functionalized SWNTs are easier to disperse in water compared to pristine SWNTs and thus are expected to be used more extensively in industrial applications involving aqueous media. The SWNT suspension (1.0 g/L) was ultrasonicated (Misonix 3000, Misonix Inc., Farmingdale, NY) twice in deionized water for a cycle of 1 h each time. The dispersed SWNTs from the second cycle were split evenly into different vials and served as stock solutions for the subsequent column experiments. The concentration of the SWNT stock solution was measured gravimetrically using an ultramicrobalance (Mettler Toledo MX5) with a repeatability of 2.5 μg.

Fullerene (C_{60}) nanoparticles were also used in the column experiments to compare the transport and filtration behavior of nearly spherical carbon-based nanomaterials to that of the more complex SWNTs. Details on the synthesis and physicochemical properties of the aqueous fullerene nanoparticles are described elsewhere (*20*).

The prepared SWNT stock solutions were adjusted to the specified electrolyte concentration and were sonicated for 10 min before injection into the packed soil column. For consistency in the experiments, the time gap between sonication and the SWNT injection into the column was kept constant (5 min) in all experiments. Hydrodynamic radii of the SWNT and fullerene nanoparticles, determined by dynamic light scattering (DLS) (ALV-5000, Langen, Germany), were 122 (±5.0) and 50.5 (±1.0) nm, respectively. Before the start of the column experiments, SWNT and fullerene concentrations were calibrated at different ionic strengths using absorbance at 210 and 344 nm, respectively (*18, 19*).

Natural Soil. The box cut soil sample was collected from the Connecticut Agricultural Experiment Station site in Hamden, CT. The soil, classified as Cheshire fine sandy loam, was originally deposited by the Wisconsin Glacier (*21*). Because this site is protected for agriculture-related research, the soil is pristine and free from contaminants. Our rationale of using near-surface soil for the column experiments is that the uppermost soil surfaces are the most probable sites for release/disposal of nanomaterials such as SWNTs.

After removal of grass roots and pebbles, the soil was oven-dried at 45 °C for 3 days. Thereafter, it was gently ground and thoroughly mixed to generate a homogeneous batch, after which it was dry-sieved to achieve soil aggregates ranging in size from 0.42 to 1.0 mm. The porosity of this size fraction soil was measured using a standard pycnometer test (*22*). Other soil properties, including grain size and pore size distribution, mineralogy, organic matter content, and hydraulic conductivity, were measured at the Penn State Materials Characterization Laboratory and the Soil Testing Laboratory at South Dakota State University.

Soil Column Packing and Conditioning. Ten-gram soil aggregates (0.42−1.00 mm) were dry-packed in a glass chromatography column (inner diameter of 1.6 cm) to a height of 4.3 cm. To achieve uniform packing, the soil was carefully deposited in the chromatography column by using a spatula and then gently vibrated. The column was slowly saturated by pumping 20 mM $CaCl_2$ solution in the upward direction at an approach velocity of 1.5×10^{-3} cm/s for 1 h. Following this saturation step, the column was conditioned by pumping 25 pore volumes of 20 mM $CaCl_2$ at an approach velocity of 3.0×10^{-3} cm/s. After this soil colloid stabilization step, the feed solution was replaced with 1 mM KCl solution. The approach velocity was then increased stepwise to attain a conditioning approach velocity of 2.2×10^{-2} cm/s. A total of at least 500 pore volumes were eluted during the conditioning step.

Following the above column conditioning and soil colloid stabilization steps, the approach velocity was adjusted to the targeted approach velocity for the column experiment. The column was further reconditioned with 50 pore volumes of the desired solution conditions (KCl or $CaCl_2$) for the SWNT deposition experiment. The amount of colloids released during the saturation and conditioning steps was continuously monitored over time (by measuring the absorbance at 210 nm). Particular attention was paid to detect possible soil colloid mobilization during increases in approach velocity or decreases in ionic strength, because these two conditions have been found to mobilize natural soil colloids (*11*). Our extensive preliminary experiments found that slow, stepwise increase in approach velocity and decrease in ionic strength were most effective in minimizing the loss of soil colloids, as well as avoiding pore clogging that results from colloid mobilization. The cumulative loss of soil colloids in any column was limited to less than 2.4 wt % of the total packed soil mass in the column.

Column Transport Experiments. The column setup consisted of a (i) reservoir containing the background electrolyte solution, (ii) peristaltic pump (MasterFlex, model 75−1920, Cole Parmer Company, Vernon Hills, IL) controlling the steady state flow rate, (iii) glass chromatography column containing the packed conditioned soil, and (iv) UV/visible spectrophotometer for online monitoring of SWNT or fullerene column effluent concentration (Hewlett-Packard Model 8453). A 250-μL pulse injection loop was connected at the column entrance. During the column experiment, a pulse of SWNTs, fullerene nanoparticles, or KBr tracer in the desired background electrolyte concentration was introduced into the column as a single-step pulse injection. A separate bypass connection, excluding the column, was employed to measure the initial concentration of the stock solution in the injection loop. The effluent concentration of SWNTs, fullerenes, or tracer from the column was monitored at 3-s intervals by measuring the absorbance at 210, 344, and 216 nm, respectively, with a UV/visible spectrophotometer and a 70-μL flow-through quartz cuvette.

Three different sets of column experiments were performed to understand the mechanisms of SWNT transport and filtration in soil media. The first set of experiments was aimed at understanding the general transport behavior of SWNTs in the packed soil column. It included the effect of approach (superficial) velocity (1.4×10^{-3} to 2.8×10^{-2} cm/s) on the deposition rate. In the second set of experiments, the mass of injected SWNTs was varied from 7 to 125 μg to test whether SWNT deposition follows first-order kinetics analogous to the deposition of other types of colloidal particles in porous media (e.g., refs *10*−*14*). The third set of experiments was performed over a range of KCl (0.1 to 100 mM) and $CaCl_2$ (0.03 to 10 mM) concentrations to understand the physicochemical mechanisms governing SWNT deposition in the packed soil column. Unless otherwise indicated, the approach velocity and mass input of SWNTs (pulse injection) were kept constant at 2.2×10^{-2} ($\pm 0.1 \times 10^{-2}$) cm/s and 65 (±5) μg, respectively. Additional column experiments with aqueous fullerene nanoparticles were also performed to better understand SWNT deposition/filtration mechanisms. All column experiments were performed with unbuffered aqueous solutions (ambient pH of 5.6−5.8). Because the packed porosity can be different from that calculated from the pycnometer test (*23*), the pore volume in our study was calculated from an identical pulse experiment conducted using a conservative tracer, KBr (*11*).

A potential problem in the packed soil column experiments is the possible migration and filtration of soil colloids that were mobilized (released) from the soil column (*24*). Migration and subsequent filtration of soil colloids can also affect the hydrodynamic properties of the packed column

and, therefore, may alter the SWNT deposition behavior. To monitor this problem, we measured the column effluent absorbance in real time to detect temporal loss of soil colloids (particularly during increases in approach velocity and decreases in ionic strength). We also collected all the eluted solution to quantify the total loss of soil mass from the packed column. To further confirm the closely identical hydrodynamic properties of each packed soil column, a tracer (KBr) run was conducted in each column immediately following the SWNT/fullerene column experiments. Only experiments from columns in which tracer breakthrough curves from different column runs closely superimposed were accepted and included for further analyses.

Determination of SWNT Deposition Rate Coefficients. The transport and deposition of nanoparticles in packed columns can be described by a one-dimensional advection−dispersion equation with a sink term for particle deposition. For a unit pulse input of particle suspension passing through a semi-infinite column initially free of any deposited particles, the solution of the one-dimensional advection−dispersion equation for the spatial and temporal distribution of the particle concentration, $C(x, t)$, at a column depth x and time t is given by (*11*, *25*, *26*):

$$C(x, t) = n_0 \frac{x}{2\sqrt{\pi t^3 D}} \exp(-k_d t) \exp\left[-\frac{(x - vt)^2}{4Dt}\right] \quad (1)$$

where n_0 is the ratio of the total amount of SWNT injected to the volumetric flow rate, v is the fluid interstitial velocity (i.e., approach velocity divided by porosity), D is the hydrodynamic dispersion coefficient, and k_d is the particle deposition rate coefficient. The SWNT breakthrough curves as a response to a pulse input were fitted to eq 1, using a nonlinear least-squares analysis, to simultaneously obtain the deposition rate coefficient (k_d) and hydrodynamic dispersion coefficient (D). Final values of k_d were obtained from fitting the measured breakthrough curves again using the average value of D.

Results and Discussion

Properties of SWNTs and Soil Media. Electrokinetic and physical properties of the SWNTs used in this study are described in detail in our recent publication (*18*). In brief, the carboxylated SWNTs are negatively charged and relatively pure (residual metal content 1.8%), with diameters ranging from 0.9 to 1.6 nm and lengths varying from 0.6 to 8 μm. Even after two phases of sonication, the SWNTs were still bundled (Figure S1). However, mechanical energy of sonication enhanced the defect level of SWNTs as indicated by Raman spectroscopy (*18*). Specifically, the G/D ratio of the as-received SWNTs decreased from 2.33 to 0.51 after sonication treatment, indicating an enhancement in defects induced by sonication. The SWNT BET surface area (supplied by the manufacturer) is 407 m^2/g.

Table 1 summarizes the key soil mineral characteristics. The soil consists of a high amount of clay-sized particles (29%) and is classified as a sandy clay loam based on the USDA soil triangle classification. As expected, the higher clay content in the soil is correlated with the low saturated hydraulic conductivity (4.62×10^{-3} cm/s). The XRD results indicate that the soil is dominated by clay minerals (kaolinite, montmorillonite, halloysite, and muscovite) and contains some quartz and feldspars, as well as a minor amount of iron oxides (Table 1). The soil is also relatively rich in organic matter (2.9%). Nitrogen BET adsorption isotherms reveal that the soil has a surface area of 3.67 m^2/g and an average pore width of 22 nm. However, the surface area calculated from packed dry soil in the BET buret is expected to be lower than that in the saturated packed soil column because of slacking of soil clumps/aggregates and swelling of clay minerals.

TABLE 1. Key Properties of the Size-Fractioned (0.42−1.0 mm) Soil Used in the Column Experiments

particle size distribution	sand (58%), silt (13%), and clay (29%)
USDA soil classification	sandy clay loam
cation exchange capacity	133.5 meq/kg
organic matter	2.9 wt %
mineralogy	clay minerals (kaolinite, montmorillonite, halloysite, muscovite), quartz and feldspars, and a minor amount of iron oxides
BET surface area	3.67 m^2/g
BJH average pore diameter	22 nm
saturated hydraulic conductivity	4.62×10^{-3} cm/s (at 20 °C)

General Transport and Deposition Behavior of SWNTs. Deposition of colloidal particles in porous media follows first-order kinetics with respect to particle concentration at the initial stages of filtration when surface coverage is low. Figure 1 demonstrates that the normalized SWNT breakthrough curves are identical for pulse input experiments involving various amounts of SWNTs (7−95 μg), thereby indicating that SWNT deposition follows first-order kinetics (*11*). This behavior also suggests that surface coverage by deposited SWNTs is quite low for SWNT pulses of less than 95 μg. The tailing in SWNT breakthrough curves is likely an experimental artifact, rather than an indication of SWNT release. This tailing is attributed to dispersion in the flow-through cuvette (*27*), as tailing is present for both the SWNT and tracer breakthrough curves (to be presented later). At higher SWNT concentrations (>95 μg, data not shown), however, the normalized breakthrough curves displayed an attenuation with increasing SWNT concentration. This behavior is likely due to aggregation of SWNTs in the column influent solution at high SWNT concentration, which results in greater filtration in the soil column.

Decreasing the flow rate (or approach velocity) resulted in attenuated SWNT concentration at the column outlet (Figure S2), as expected according to filtration theory (*28*). SWNT deposition rate coefficients, determined from fitting the breakthrough curves to eq 1, are shown in Figure 2 for a range of approach velocities. The results show that the logarithm of the deposition rate coefficient increases linearly

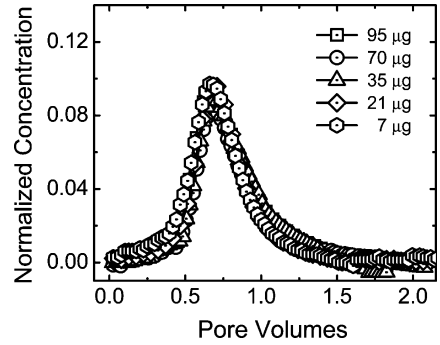

FIGURE 1. Normalized SWNT breakthrough curves at 1 mM KCl for different amounts of SWNTs introduced to the packed soil column as pulse input. Experimental conditions: column length = 4.3 cm, approach velocity = 0.022 (±0.001) cm/s, porosity = 0.58, pH = 5.6−5.8, and temperature = 22−23 °C. Properties of the soil used in the column experiments are described in Table 1. Normalized concentration refers to the measured mass concentration of SWNTs at the column outlet divided by the ratio of total amount of injected SWNTs (indicated in figure) to the volume of the injected pulse (250 μL).

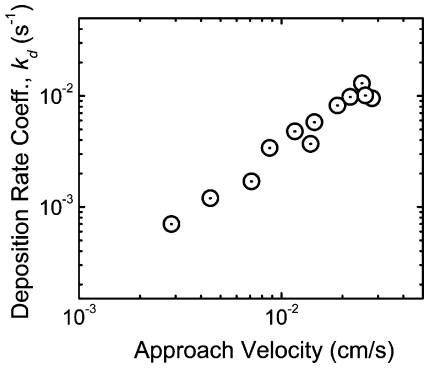

FIGURE 2. Influence of approach velocity on SWNT deposition rate. All experiments were performed with a pulse input of 65 (±5) μg of SWNTs and a background electrolyte concentration of 1 mM KCl. Other experimental conditions are similar to those described in Figure 1.

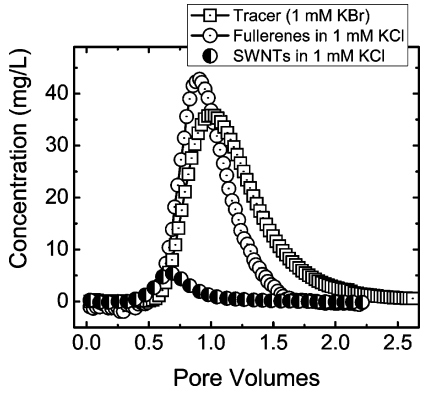

FIGURE 3. General transport behavior of SWNTs and fullerene nanoparticles in the packed soil column in comparison to an inert tracer (KBr). The total mass of SWNTs and fullerenes used in each experiment was 65 (±5) μg. Other experimental conditions are similar to those described in Figure 1.

with the logarithm of approach velocity, with a slope of 0.65 (R^2 = 0.95). This slope is comparable to that found for deposition of soil-mobilized colloids in the parental soil matrix (i.e., $k_d \propto v^{0.6}$, with v being the approach velocity) (*11*). For impermeable collectors, such as quartz sand and glass beads, the predicted power dependence for spherical, Brownian particles undergoing deposition by a convective−diffusive mechanism is 1/3 (i.e., $k_d \propto v^{1/3}$) (*28, 29*). Our results in Figure 2 may suggest that the SWNTs in the soil column are not predominately removed by classical physicochemical filtration mechanisms, such as deposition by convective-diffusion, but rather by straining as discussed later in the paper.

Size Exclusion of SWNTs in Flow through Soil. In all cases studied, SWNT (and fullerene) breakthrough occurred considerably ahead of that of the KBr tracer as seen from the peaks or center of mass of the breakthrough curves (Figure 3). This phenomenon, known as size exclusion chromatography (*11, 14*), has been reported for transport of colloidal particles and macromolecules, where colloid breakthrough occurs before that of low molecular weight tracer because colloidal particles are excluded from small pores. The observed size exclusion effect occurs because many continuous pores in the soil, where tracer can pass through, are too small for SWNTs and fullerene nanoparticles to pass through. As a result, the tracer pathways are longer and have larger tortuosity than that of the nanomaterials. Our results, calculated from the position of the center of mass or peak in the breakthrough profile (Figure 3), show that the exclusion volumes of the total pores or the time delays of the breakthrough profiles are dependent on the size of the nanomaterial: about 10% for fullerenes (50.5 nm) and 27% for SWNTs (122 nm) compared to KBr tracer. The irregular shape, large aspect ratio, and size distribution of SWNTs may also have contributed to an increase in the size exclusion effect.

We note that size exclusion effect was insignificant in our previous study (*18*) involving transport of similar SWNTs in columns packed with uniform sand grains (263 μm in diameter), indicating that the soil matrix played an important role in the transport behavior of SWNTs. The soil used in our study was microporous in nature with an average pore diameter of 22 nm (Table 1). Furthermore, the pore size distribution was more skewed toward the smaller size range, with 40% of the pores being less than 10 nm wide. Consequently, SWNTs are excluded from these pores due to their large size and slow diffusion compared to water and tracer. However, we caution that the pore size distribution of soil particles obtained from nitrogen sorption/desorption isotherms using a soil packed in the BET buret may not reflect the actual pore size distribution in the wet packed soil column.

SWNT Deposition Kinetics in Monovalent Salt. Typical SWNT breakthrough curves over a wide range of KCl concentrations are presented in Figure 4a. The deposition rate coefficients calculated from such breakthrough curves are shown in Figure 4b. Overall, the deposition of SWNTs in the soil column increases with increasing KCl concentration, consistent with previous studies on particle deposition in soil columns (*11, 14*). However, even at low salt concentration (1 mM KCl), a significant fraction of SWNTs (~80%) was retained in the column (Table S1, Supporting Information). Notably, at low and intermediate ionic strengths, the SWNT deposition rate coefficients are 1 order of magnitude higher than those observed in our recent study with the same SWNTs being deposited in a column packed with uniform sand grains (*18*).

The type of soil minerals and their properties also affect SWNT deposition. As shown in Table 1, the soil is composed predominately of clay minerals, such as kaolinite, montmorillonite, halloysite, and muscovite. Broken edges of clay minerals containing Si−O−Si and Al−O−Al moieties result in pH-dependent ionizable silanol (Si−OH) and aluminol (Al−OH) functional groups. Many clay minerals have point of zero charge (PZC) at or near neutral pH (*30, 31*). Since the pH chosen in this study (pH 5.5−5.8) was lower than the PZC of iron oxides and clay minerals, the soil is expected to have a small fraction of positively charged sites, which may influence SWNT retention in the soil columns. However, the minor fraction of iron oxides (Table 1) likely plays an insignificant role in SWNT deposition, as otherwise we would have obtained high retention of fullerene nanoparticles at low ionic strengths, which was not the case observed (Table S1 and discussion later in the paper).

SWNT Deposition Kinetics in Divalent Salt. Natural soil environments contain a significant amount of soluble Ca^{2+}, resulting primarily from dissolution of carbonates and calcic bedrocks. The influence of calcium ion concentration on SWNT breakthrough curves and the corresponding deposition rate coefficients are shown in Figure 5. As expected, an increase in Ca^{2+} concentration enhances SWNT filtration in the soil column. However, the deposition rate is already very high, even at extremely low (0.03 mM) $CaCl_2$ concentration, and the change in deposition rate over a 3 orders of magnitude increase in calcium ion concentration is relatively small.

Straining Governs SWNT Filtration. Straining, the trapping of particles in pores that are too small to allow particle passage, normally occurs when the ratio of the particle to collector grain diameters is greater than 0.003 (*32*). This ratio has been found to be as low as 0.0008 during transport of asymmetrical and highly bundled SWNTs (based on hydro-

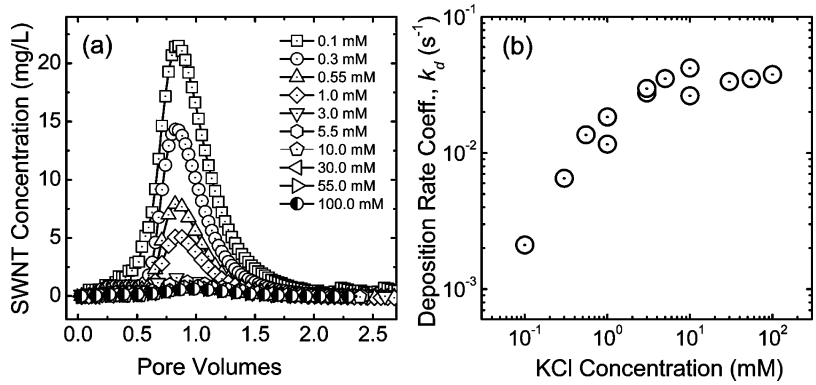

FIGURE 4. (a) SWNT breakthrough curves at various KCl concentrations for runs with the packed soil columns. (b) Calculated deposition rate coefficients, k_d, of SWNTs for column runs at various KCl concentrations. The total mass of SWNTs used in each experiment (as a pulse input) was 65 (±5) μg. Other experimental conditions are similar to those described in Figure 1. The average hydrodynamic dispersion coefficient (D) of SWNTs in the soil column was 4.32 × 10^{-3} cm^2/s.

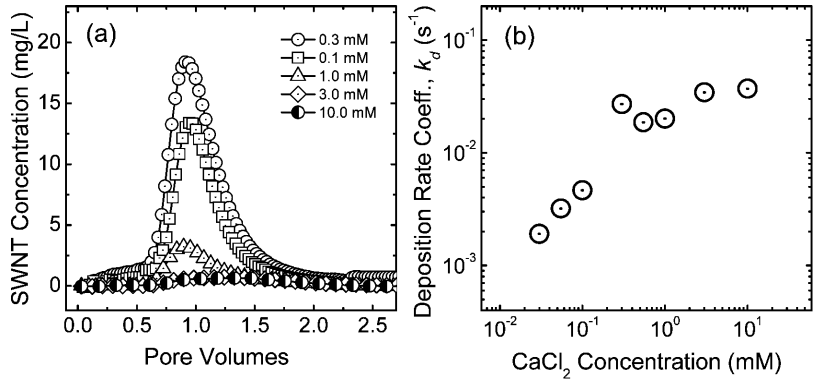

FIGURE 5. (a) SWNT breakthrough curves at various $CaCl_2$ concentrations for runs with the packed soil columns. (b) Calculated deposition rate coefficients, k_d, of SWNTs for column runs at various $CaCl_2$ concentrations. The total mass of SWNTs used in each experiment (as a pulse input) was 65 (±5) μg. Other experimental conditions are similar to those described in Figure 1.

dynamic diameter) in a well-defined porous medium composed of clean quartz sand (*18*). Our results show that the SWNT deposition rate coefficients (k_d) are quite high, even at very low salt concentrations (Figures 4b and 5b, Table S1). Furthermore, k_d did not change appreciably above 0.3 mM KCl or 0.1 mM $CaCl_2$. Since electrostatic double layer repulsion between SWNTs and soil grains is expected to be very high at such low salt concentrations, deposition of SWNTs is expected to be very low. These observations suggest that straining plays an important role in the deposition of SWNTs in our soil columns.

To further verify our hypothesis that straining is a dominant mechanism of SWNT deposition, similar experiments were conducted using nearly spherical fullerene nanoparticles in columns packed with the same soil. Fullerene nanoparticles are smaller, with a hydrodynamic radius of 50.5 (±1.0) nm and an aspect ratio of unity, compared to 122 (±5.0) nm for SWNTs (with an aspect ratio as high as 1000, Figure S1 and ref *18*). Fullerene deposition rate coefficients are much lower than those of SWNTs at the same ionic strength (Figure 6, Table S1). Furthermore, the deposition rate of fullerene nanoparticles is more sensitive to changes in ionic strength compared to that of SWNTs. Note, however, that the SWNT deposition rate also increases, albeit slowly, with increasing ionic strength. This result suggests that physicochemical filtration plays some role in the retention of SWNTs in saturated soil media at low ionic strengths.

Pore size distribution and pore geometry likely control the transport and filtration of SWNTs in the soil column. Since the soil used in the column experiments consisted primarily of small pores (Table 1), both SWNTs and fullerene nanoparticles were expected to encounter straining but to a different extent. Our results indicate that physical straining

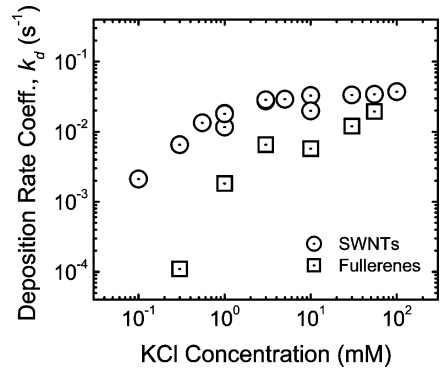

FIGURE 6. Comparison of deposition rate coefficients of SWNTs and fullerene nanoparticles (C_{60}) as a function of KCl concentration. All experiments were performed in identical packed soil columns as described in Figure 1. The total mass of SWNTs and fullerenes in each experiment (as a pulse input) was kept constant at 65 (±5) μg.

plays a predominant role in SWNT filtration for all ranges of ionic strengths and solution chemistries used in the present study. It is proposed that SWNT shape and structure, particularly the very large aspect ratio and its highly bundled (aggregated) state in aqueous solutions, as well as heterogeneity in soil particle size, porosity, and permeability, collectively contribute to straining in flow through soil media.

Implications for Transport of SWNTs in Soil Environments. The maximum travel distance of SWNTs, defined here as the distance required before 99.9% of influent SWNTs are filtered out, can be calculated from the measured k_d values using filtration theory. Such calculations indicate that SWNT

transport is limited to 5.5 and 4.6 cm at 1 and 10 mM KCl, respectively. However, natural soil environments are more heterogeneous and normally contain open soil structures (e.g., cracks, fissures, worm trails, and other open features) that can promote preferential flow of SWNTs in soil. Similarly, soil porewater is normally rich in dissolved organic molecules (e.g., soluble organic matter and humic and fulvic acids) that can enhance the colloidal stability of nanomaterials and, therefore, increase their travel distances. Regardless, our study suggests that compared to other types of colloidal particles and nanomaterials, SWNT transport in soils would be limited and may not pose a risk in contaminating underlying groundwater aquifers. Moreover, commercial SWNTs may be more bundled and aggregated than the treated (sonicated) SWNTs used in this study, which would further enhance their retention in soils.

Acknowledgments

Support for D. P. Jaisi was provided by the Yale University Interdepartmental Bateman Postdoctoral Fellowship. We thank Joseph Pignatello and Jason White for allowing the use of soil material from the Connecticut Agricultural Experimental Station in Hamden, CT. We also acknowledge the support of the National Science Foundation under Research Grant CBET-0828795.

Supporting Information Available

Summary of deposition data for SWNTs and fullerene nanoparticles for column experiments with KCl and $CaCl_2$ (Table S1). TEM image of SWNTs showing a representative long and folded bundle of nanotubes (Figure S1). SWNT breakthrough curves for column experiments with packed soil at different approach velocities (Figure S2). This material is available free of charge via the Internet at http://pubs.acs.org.

Literature Cited

(1) Hu, Y.; Shenderova, O.; Brenner, D. Carbon nanostructures: Morphologies and properties. *J. Comput. Theor. Nanosci.* **2007**, *4*, 199–221.
(2) Mauter, M. S.; Elimelech, M. Environmental applications of carbon-based nanomaterials. *Environ. Sci. Technol.* **2008**, *42*, 5843–5859.
(3) Balasubramanian, K.; Burghard, M. Chemically functionalized carbon nanotubes. *Small* **2005**, *1*, 180–192.
(4) Nowack, B.; Bucheli, T. D. Occurrence, behavior and effects of nanoparticles in the environment. *Environ. Pollut.* **2007**, *150*, 5–22.
(5) Perez, S.; Farre, M.; Barcelo, D. Analysis, behavior and ecotoxicity of carbon-based nanomaterials in the aquatic environment. *TrAC, Trends Anal. Chem.* **2009**, *28*, 820–832.
(6) Lam, C.-W.; James, J. T.; McCluskey, R.; Hunter, R. L. Pulmonary toxicity of single-wall carbon nanotubes in mice 7 and 90 days after intratracheal instillation. *Toxicol. Sci.* **2004**, *77*, 126–134.
(7) Kang, S.; Pinault, M.; Pfefferle, L. D.; Elimelech, M. Single-walled carbon nanotubes exhibit strong antimicrobial activity. *Langmuir* **2007**, *23*, 8670–8673.
(8) Pulskamp, K.; Diabate, S.; Krug, H. F. Carbon nanotubes show no sign of acute toxicity but induce intracellular reactive oxygen species in dependence on contaminants. *Toxicol. Lett.* **2007**, *168*, 58–74.
(9) Guzman, K. A.; Taylor, M. R.; Banfield, J. F. Environmental risks of nanotechnology: National Nanotechnology Initiative funding, 2000−2004. *Environ. Sci. Technol.* **2006**, *40*, 1401–1407.
(10) Kuhnen, F.; Bhattacharjee, S.; Elimelech, M.; Kretzschmar, R. Transport and deposition dynamics of iron oxide colloids in packed quartz media: monolayer and multilayer deposition. *J. Colloid Interface Sci.* **2000**, *231*, 32–41.
(11) Grolimund, D.; Elimelech, M.; Borkovec, M.; Barmettler, K.; Kretzschmar, R.; Sticher, H. Transport of in situ mobilized colloidal particles in packed soil columns. *Environ. Sci. Technol.* **1998**, *32*, 3562–3569.
(12) Redman, J. A.; Walker, S. L.; Elimelech, M. Bacterial adhesion and transport in porous media: role of the secondary energy minimum. *Environ. Sci. Technol.* **2004**, *38*, 1777–1785.
(13) Ryan, J. N.; Elimelech, M. Colloid mobilization and transport in groundwater. *Colloids Surf.* **1996**, *107*, 1–56.
(14) Kretzschmar, R.; Borkovec, M.; Grolimund, D.; Elimelech, M. Mobile subsurface colloids and their role in contaminant transport. *Adv. Agron.* **1999**, *66*, 121–193.
(15) Lecoanet, H. F.; Wiesner, M. R. Velocity effects on fullerene and oxide nanoparticle deposition in porous media. *Environ. Sci. Technol.* **2004**, *38*, 4377–4382.
(16) Lecoanet, H. F.; Bottero, J. Y.; Wiesner, M. R. Laboratory assessment of the mobility of nanomaterials in porous media. *Environ. Sci. Technol.* **2004**, *38*, 5164–5169.
(17) Wang, Y. G.; Li, Y. S.; Pennell, K. D. Influence of electrolyte species and concentration on the aggregation and transport of fullerene nanoparticles in quartz sands. *Environ. Toxicol. Chem.* **2008**, *27*, 1860–1867.
(18) Jaisi, D. P.; Saleh, N. B.; Blake, R. E.; Elimelech, M. Transport of single-walled carbon nanotubes in porous media: filtration mechanisms and reversibility. *Environ. Sci. Technol.* **2008**, *42*, 8317–8323.
(19) Li, Y. S.; Wang, Y. G.; Pennell, K. D.; Abriola, L. M. Investigation of the transport and deposition of fullerene (C60) nanoparticles in quartz sands under varying flow conditions. *Environ. Sci. Technol.* **2008**, *42*, 7174–7180.
(20) Chen, K. L.; Elimelech, M. Relating colloidal stability of fullerene (C60) nanoparticles to nanoparticle charge and electrokinetic properties. *Environ. Sci. Technol.* **2009**, *43*, 7270−7276.
(21) Uchupi, E.; Driscoll, N.; Ballard, R. D.; Bolmer, S. T. Drainage of late Wisconsin glacial lakes and the morphology and late quaternary stratigraphy of the New Jersey-southern New England continental shelf and slope. *Marine Geol.* **2001**, *172*, 117–145.
(22) ASTM D-1480. Standard test method for density and relative density (specific gravity) of viscous materials by bingham pycnometer, American Society of Testing Materials, West Conshohocken, PA, 2007.
(23) Sardin, M.; Schweich, D.; Leij, F. J.; van Genuchten, M. T. Modeling the non-equilibrium transport of linearly interacting solutes in porous-media - a review. *Water Resour. Res.* **1991**, *27*, 2287–2307.
(24) Dikinya, O.; Hinz, C.; Aylmore, G. Decrease in hydraulic conductivity and particle release associated with self-filtration in saturated column. *Geoderma* **2008**, *146*, 192–200.
(25) Chen, J. Y.; Ko, C.-H.; Bhattacharjee, S.; Elimelech, M. Role of spatial distribution o porous medium geochemical heterogeneity in colloid transport. *Colloid Surf., A* **2001**, *191*, 3–16.
(26) Ketzschmar, R.; Barmettler, K.; Grolimund, D.; Yan, Y. D.; Borkovec, M.; Sticher, H. Experimental determination of colloid deposition rates and collision efficiencies in natural porous media. *Water Res.* **1997**, *33*, 1129–1137.
(27) Weronski, P.; Walz, J. Y.; Elimelech, M. Effect of depletion interaction on transport of colloidal particles in porous media. *J. Colloid Interface Sci.* **2003**, *262*, 372–383.
(28) Tufenkji, N.; Elimelech, M. Correlation equation for predicting single-collector efficiency in physicochemical filtration in saturated porous media. *Environ. Sci. Technol.* **2004**, *38*, 529–536.
(29) Song, L. F.; Elimelech, M. Calculation of particle deposition rate under unfavorable particle surface interactions. *J. Chem. Soc., Faraday Trans.* **1993**, *89*, 3443–3452.
(30) Herrington, T. M.; Clarke, A. Q.; Watts, J. C. The surface charge of kaolin. *Colloids Surf.* **1992**, *68*, 161–169.
(31) Jaisi, D. P.; Liu, C.; Dong, H.; Blake, R. E.; Fein, J. Fe^{2+} sorption onto nontronite (NAu-2). *Geochim. Cosmochim. Acta* **2008**, *72*, 5361–5371.
(32) Bradford, S. A.; Torkzaban, S.; Walker, S. L. Coupling of physical and chemical mechanisms of colloid straining in saturated porous media. *Water Res.* **2007**, *41*, 3012–3024.

ES901927Y